

This is the pdf of the article published in *Advanced Electronic Materials* on 26 October 2022
<https://doi.org/10.1002/aelm.202200613>

Ultrafast Racetrack Based on Compensated Co/Gd-Based Synthetic Ferrimagnet with All-Optical Switching

Pingzhi Li,* Thomas J. Kools, Bert Koopmans, and Reinoud Lavrijsen

Spin-orbitronics and single pulse all-optical switching (AOS) of magnetization are two major successes of the rapidly advancing field of nanomagnetism in recent years, with high potential for enabling novel, fast, and energy-efficient memory and logic platforms. Fast current-induced domain wall motion (CIDWM) and single shot AOS have been individually demonstrated in different ferrimagnetic alloys. However, the stringent requirement for their composition control makes these alloys challenging materials for wafer scale production. Here, fast CIDWM and energy efficient AOS in a synthetic ferrimagnetic system based on multilayered [Co/Gd]₂ are simultaneously demonstrated. First, it is shown that AOS is present in its full composition range. It is found that current-driven domain wall velocities over 2000 m s⁻¹ at room temperature, achieved by compensating the total angular momentum through layer thickness tuning. Furthermore, analytical modeling of the CIDWM reveals that Joule heating needs to be treated transiently to properly describe the CIDWM for our sub-ns current pulses. The studies establish [Co/Gd]-based synthetic ferrimagnets to be a unique materials platform for domain wall devices with access to ultrafast single pulse AOS.

1. Introduction and Results

Research in spintronics^[1,2] over the last decades has demonstrated a possibility for further evolution of solid-state electronic application platforms beyond CMOS. The racetrack memory,^[3] an envisioned novel data storage device concept based on using magnetic domain walls (DWs),^[4] utilizes frontier spintronic mechanisms to function as an ultra-dense on-chip memory with an operation speed comparable to low-level cache.^[5] The efficiency of racetrack memory relies on the fast CIDWM in a material with perpendicular magnetic anisotropy. The maximum velocity was significantly enhanced over the years by combining spin-orbit torques (SOTs) and

the Dzyaloshinskii–Moriya interaction (DMI)^[6–8] with synthetic antiferromagnets (SAFs), which resulted in reported DW velocities close to 750 m s⁻¹.^[9]

Despite the large improvement, the energy efficiency is still limited due to the weak strength of the antiferromagnetic (AF) coupling. Therefore, the materials platform of rare earth (RE)-transition metal (TM) compounds garnered considerable attention,^[1] promising faster CIDWM due to the much stronger direct AF coupling than the indirect exchange coupling^[10] utilized in SAFs. Furthermore, the SOTs used to drive the DW promise to be highly efficient in the RE-TM systems as a result of the long spin coherence length.^[11] Consequently, high velocity CIDWM has been reported in Co-Gd-based ferrimagnetic alloy systems^[12,13] when the angular momentum in the magnetic material is compensated, being at least a factor of three faster than that of


the previously reported SAFs.

Besides the efficient CIDWM, single pulse all-optical switching (AOS) of the magnetization^[14,15] in the RE-TM systems has obtained significant attention thanks to its sub-picosecond^[16] energy efficient^[14,17,18] magnetization switching enabled by the ultrafast angular momentum transfer upon laser excitation.^[19] This can be useful as a new generation of ultrafast magnetic memory, as well as a data buffer between electronics and integrated photonics.^[14,20,21] Recently, a synthetic ferrimagnetic system based on a Pt/Co/Gd^[18,22] layered structure has shown high robustness^[23] for such a hybrid integration.

These kinds of synthetic ferrimagnets have some distinct advantages over RE-TM alloys. For instance, AOS is not limited by the exact composition.^[24] They also withstand thermal annealing^[25] and offer easier magnetic composition control at wafer scale than the alloy system, as well as better access to interface engineering. Therefore, it has been proposed that such a materials platform has high potential to realize a hybrid integration of DW memory in photonic platforms to further enhance their storage density.^[20,26]

So far, the CIDWM of Co/Gd bilayers^[26,27] has been investigated. However, the highest reported velocity, achieved at cryogenic conditions,^[27] was several times lower than that reported in alloys,^[12] in part due to large net angular momentum, low compensation temperature as well as DW pinning effects. In this report, we therefore propose a materials platform based on the [Co/Gd]₂ synthetic ferrimagnet capable of accommodating both efficient CIDWM of over 2 km s⁻¹) at room temperature

P. Li, T. J. Kools, B. Koopmans, R. Lavrijsen
 Department of Applied Physics
 Eindhoven University of Technology
 Eindhoven 5612 AZ, The Netherlands
 E-mail: p.li1@tue.nl

 The ORCID identification number(s) for the author(s) of this article can be found under <https://doi.org/10.1002/aelm.202200613>.

© 2022 The Authors. *Advanced Electronic Materials* published by Wiley-VCH GmbH. This is an open access article under the terms of the Creative Commons Attribution License, which permits use, distribution and reproduction in any medium, provided the original work is properly cited.

DOI: 10.1002/aelm.202200613

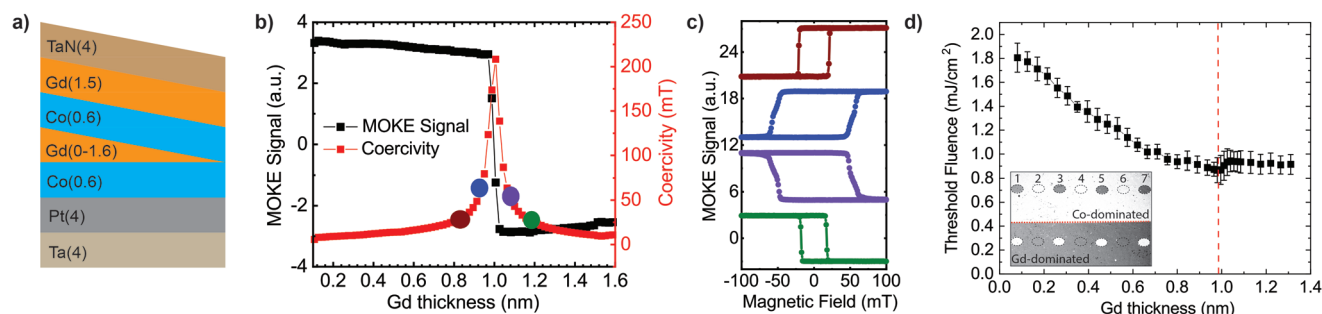


Figure 1. a) Schematic illustration of the layer stack used in our study (thickness in nm). b) Result of static MOKE study, where the MOKE signal (black) is defined by the difference in signal intensity between saturation at positive and negative applied field. Coercivity (red) was measured at a fixed scanning speed of 10 mT s^{-1} (red). c) Hysteresis loops measured at the sample thicknesses marked by the coloured dots in (b). d) Threshold fluence for all-optical switching across the wedge shown in (a). Inset shows toggle switched domains at two sides of the compensation thickness for varying amount of subsequent pulses.

(RT) on par with the state-of-the-art^[9,12,28] and single-pulse AOS, with compatibility for wafer scale production as well as robustness for engineering, which is compatible with the back-end-of-line integration technology in CMOS industry.

The magnetostatic and AOS properties of the $[\text{Co}/\text{Gd}]_2$ materials platform under investigation in this work are shown in **Figure 1**. A Ta/Pt/ $[\text{Co}/\text{Gd}]_2/\text{TaN}$ multilayer is deposited on a Si/SiO₂ substrate, where the first Gd layer is wedged (see **Figure 1a** and Experimental Section) to tune the net magnetic moment. Due to the proximity effect by the Co, a net magnetization is induced in the Gd which drops off steeply away from the Co interface.^[29] Compared to the bilayer Co/Gd,^[22,27] we double the magnetic volume of the Co in $[\text{Co}/\text{Gd}]_2$, while tripling the number of interfaces at which magnetization is induced in the Gd. This allows us to more easily compensate both the angular momentum and magnetic moment of the system at RT by varying the individual layer thicknesses.

We measured hysteresis loops by polar magneto-optical Kerr effect (MOKE) at RT across the thickness range of Gd between 0–1.6 nm. In **Figure 1b**, we plot the MOKE signal intensity, defined as the difference in signal between positive and negative saturation, as well as the coercivity obtained from these hysteresis loops. The loops corresponding to the colored dots in **Figure 1b** are presented in **Figure 1c**.

The 100% remanence indicates a well-defined perpendicular magnetic anisotropy as well as tight exchange coupling between the layers. Importantly, at the Gd thickness of 0.97 nm, the MOKE signal switches sign (see black curve in **Figure 1b**). This can be observed as well in **Figure 1c** as an inverted hysteresis loop. At this thickness the magnetization is compensated, i.e., the Co and Gd magnetization cancel each other. This is further evidenced by the divergence in coercivity, and confirmed by superconducting quantum interference device measurements (see Appendix A, Supporting Information). Thus, upon increasing the thickness of Gd, the magnetic balance is shifted from being Co-dominated to Gd-dominated.

With respect to the magnetostatics, we note that the magnetization and angular momentum compensation thickness in these $[\text{Co}/\text{Gd}]$ -based ferrimagnets are similar but not identical due to the different Landé g -factors of Co (≈ 2.2) and Gd (≈ 2.0). Therefore, when discussing compensation without further specification in the remainder of this text, we refer to angular

momentum compensation as this is the relevant condition for efficient CIDWM.^[12,27,30]

To investigate whether our 4-layer Co/Gd system is all-optically switchable, and how it depends on compensation conditions, we performed AOS experiments by illuminating the wedge with single femtosecond laser pulses with varying pulse energy, and examined the sample under a polar Kerr microscope. We find that single pulse AOS is present at every thickness on the $[\text{Co}/\text{Gd}]_2$ wedge. An example of the resulting toggle switched domains around the compensation boundary is shown in the inset of **Figure 1d**, which can be observed from the contrast inversion (see Appendix B, Supporting Information, for more images). This distinct feature that the AOS occurs both in the deep Co-dominated and Gd-dominated composition is unlike that of alloys^[17] and Co/Tb multilayers,^[31] in which AOS is only present within $\pm 1.5\%$ of the composition window. This shows the flexibility of our system in terms of AOS engineering.

We further plot the threshold fluence as a function of Gd thickness, calculated from the switched area and the corresponding pulse energy,^[22] in **Figure 1d**. We find that the threshold fluence depends significantly on the material composition, and is at a minimum around the compensation point. Initially, the threshold fluence decreases monotonously with Gd thickness up to 1 nm, with a reduction of the threshold fluence of $>50\%$ reaching 0.9 mJ cm^{-2} , which corresponds to 25 fJ for a 50^2 nm^2 domain. Such a switching energy is an order of magnitude lower than that of typical SOT and spin-transfer torque switching of a ferromagnet.^[32]

Although a full dissection of the exact mechanism behind the thickness-dependence of the threshold fluence is beyond the scope of this work, we note that previous studies have shown that reducing the Curie temperature of layered systems can lead to a reduction of the threshold fluence.^[18,22,24,33] In our case, as the Gd layer increases, the Curie temperature of the total stack is expected to drop, because the mutual exchange stabilization of the two Co layers is weakened, leading to a reduction of threshold fluence.

With compensation and AOS at RT confirmed, in the remainder of this work we demonstrate and explain the DW velocities of over 2000 m s^{-1} , as achieved in $[\text{Co}/\text{Gd}]_2$. In the case of such an AF-coupled system with DMI, two contributions

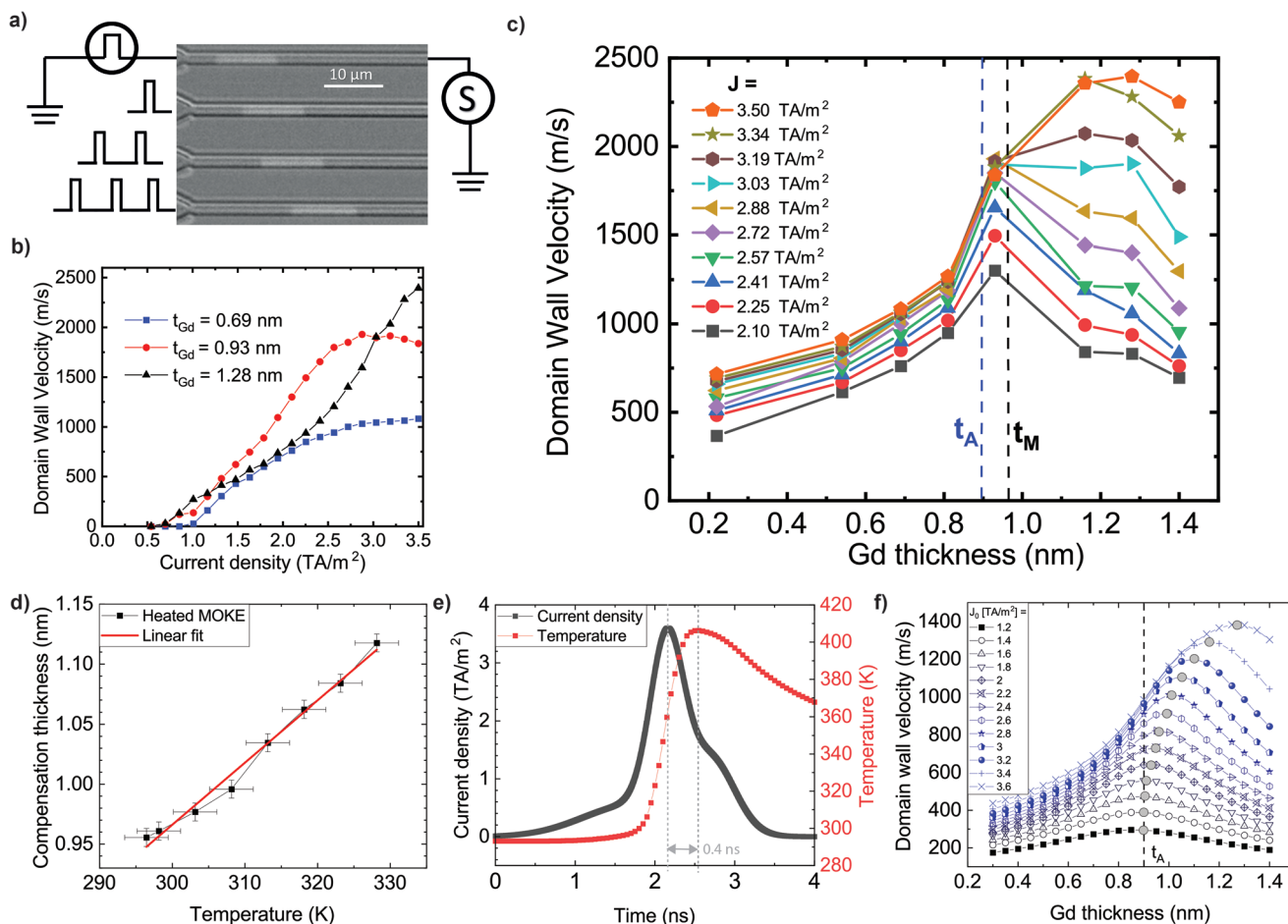


Figure 2. a) Example image from DW motion experiments performed by differential polar Kerr microscopy, where the setup is illustrated schematically as a pulse generator and a 6 GHz bandwidth oscilloscope. The DW position after applying consecutive pulses is shown. b) The measured DW velocity as a function of current density for three Gd layer thicknesses. c) The DW velocity as a function of Gd layer thickness for various current densities, where 10 % error bars are not shown. Here, we marked the quantified magnetization compensation thickness t_M obtained from polar MOKE measurements as well as the corresponding angular momentum compensation thickness t_A based on the estimation from magnetometry measurement. d) Compensation thickness as obtained from polar MOKE measurements of the $[\text{Co}/\text{Gd}]_2$ at various ambient temperatures. e) The temporal profile of the current pulse used in the experiment (normalized by the peak current density), and its subsequent temperature rise (as simulated with COMSOL) at 3.6 TA m^{-2} . f) Result of the theoretical 1D modeling: the DW velocity as a function of Gd thickness, where the magnetization profile as well as its temperature dependence is in line with experiment, while the current pulse and temperature profile follow the profile given in (d). The velocity maximum is marked with a grey dot. The vertical dashed line indicates the angular momentum compensation thickness.

mainly drive the coherent motion of the DW—the DMI-torque and the exchange coupling torque. These two torques give rise to spin dynamics upon excitation by the spin Hall-effect-induced spin accumulation, and both lead to DW motion along the current direction (for positive DMI and spin Hall angle^[7,34]).

It is well understood that the exchange coupling torque only drives the DW motion efficiently near the compensation point.^[9,27] Adding additional AF-coupled layers to a ferromagnet can facilitate this, however, can also increase the angular momentum of the DW to be translated. Nonetheless, following the discussion in Supporting information, Section C, describing an analytical study based on the well-known 1D model for domain wall motion,^[9,35] we still expect a significant increase of the DW velocity in our study, as the enhancement of exchange coupling torque due to compensation significantly overwhelms the effect of added magnetic inertia.

For this reason, we experimentally determined the DW velocity from the CIDWM in $[\text{Co}/\text{Gd}]_2$ as a function of lower Gd thickness. This study is performed in the same stack showcased in Figure 1a. The wedged thin film was patterned into micro-structures as shown in Figure 2a (for details see Experimental Section and Figure E4b, Supporting Information). The magnetic domains were imaged by polar Kerr microscopy (see Figure 2a). Short current pulses of $\approx 1 \text{ ns}$ duration with varying amplitudes are injected into the structures to determine the DW velocity (see Appendix D, Supporting Information). We observe that the DW moves coherently along the current direction (see Figure 2a). This confirms a left-handed Néel-type DW in our system as a result of a positive DMI, and a positive spin Hall angle,^[7,34] as is characteristic of the Pt–Co interface.^[7]

In Figure 2b, we compare the resulting DW velocity as a function of peak current density for a Co-dominated (0.69 nm),

compensated (0.93 nm) and Gd-dominated stack (1.28 nm), considering the magnetic composition at RT. We demonstrate that DW velocities of over 2000 m s⁻¹ can be achieved at the highest current densities, at least three times larger than that observed in SAFs.^[9]

Furthermore, we notice from the crossing point between the red and black curve that the Gd thickness at which the highest velocity is observed becomes larger with increasing current density. We attribute this to the effect of Joule heating induced by the current pulses. Earlier studies show that the Gd magnetization is quenched more severely during Joule heating than that of Co.^[27–29,36] The consequence is that at higher temperature relatively more Gd than at RT is needed to achieve compensation. This fact is confirmed for our stacks by the upward shift of the compensation thickness with increasing sample temperature using polar MOKE (see Figure 2d). We find that this hypothesis of a Joule-heating-induced shift of the compensation thickness explains the CIDWM experiments well. To understand this, it useful to consider two regimes in Figure 2b in more detail.

For $J < 2.3 \text{ TA m}^{-2}$, before saturation effects start to occur and for limited heating, we observe a steady rise of the velocity, consistent with earlier work on CIDWM in materials with AF coupling. As expected, the compensated sample is driven most efficiently. We visualize this further by plotting the DW velocity as a function of Gd thickness across the Co and Gd-dominated regimes, as is shown in Figure 2c. Here, we observe that the DW velocity in this range of current densities spikes at the RT compensation thickness, further proving the origin of the velocity increase is due to the enhanced exchange coupling torque.

for the Co-dominated and the compensated sample. This is typical behavior of the CIDWM of a ferromagnet,^[7,9,27,34,37] which is limited by the DMI-torque. Contrarily, the Gd-dominated sample shows a consistent velocity rise typically associated with a compensated system.^[9] This is consistent with the hypothesis that the increased Joule heating shifts the compensation point to larger Gd thicknesses during the pulse, and is supported by the velocity peak shift observed in Figure 2c.

In order to quantify the effect of the change in compensation thickness due to Joule heating on the CIDWM, we first numerically investigate the temperature transient for the current pulses applied in the experiment (see Appendix E, Supporting Information). In Figure 2e, we plot a typical current density profile and the corresponding modelled temperature change in the device. We observe a delay of $\approx 0.4 \text{ ns}$ between the peak current density, and the peak temperature. This is a consequence of the fact that the pulse duration approaches the characteristic time scale of the heat transport between the sample and the substrate (See Appendix E, Supporting Information).

Importantly, around the peak current density where the driving torque exerted on the DW is largest, the sample temperature is changing rapidly from 0 to 50 % of maximum temperature within 0.4 ns. Therefore, the net angular momentum changes rapidly during the application of the pulse. This makes assigning an effective temperature during DW motion like previous studies^[12,27,28,38] inaccurate.

Therefore, we incorporated the transient current density profile, and the corresponding temperature rise into an analytical 1D model of the CIDWM (see Appendix F, Supporting

Information), where we introduce a thickness and temperature-dependent magnetization profile following our SQUID measurements (see Appendix A, Supporting Information). The resulting modeled DW velocity as a function of thickness and current density is plotted in Figure 2f.

We find that the velocity peak shift with increased current density as shown in Figure 2b is well described by our model. Furthermore, we also find that the rapidly changing angular momentum during the current pulse gives rise to a broadening of the velocity peak compared to the case with constant temperature previously described in^[12,27] (see Appendix G, Supporting Information).

These results suggest that in general transient treatment of the temperature profile is necessary to properly address the DW dynamics for ultrashort current pulses. Furthermore, to benefit from large exchange coupling torque at elevated temperature, which is a likely scenario in high-speed electronics, pushing the composition into the Gd-dominated regime is required.

2. Conclusion

In summary, we have presented a materials platform of a synthetic ferrimagnet based on [Co/Gd]₂ that can be effectively tuned near the compensation point via layer thickness, and exhibits efficient single pulse AOS. We also experimentally and numerically showed that fast CIDWM with velocities over 2000 m s⁻¹ can be achieved with the help of angular momentum compensation. Finally, we addressed the transient Joule heating effect during CIDWM, which gives important insight into our experimental observations and potential technological implementation. Our results therefore lay the foundation for an effective materials platform that exhibits both ultrafast CIDWM and AOS, paving the way for synthetic ferrimagnets to become the new paradigm of ferrimagnetic spintronics and providing a jumping board for further integration between photonics and spintronics.

3. Experimental Section

Magnetic films were deposited on Si substrates with a 100 nm thermally oxidized SiO₂ layer by D.C. magnetron sputtering in a system with a base pressure of $\approx 5 \times 10^{-9} \text{ mBar}$. A thickness wedge is created with the help of a moving wedge shutter during sputtering. From these thin films, nanostrips were fabricated using electron-beam lithography and lift-off. The gold contacts were made by wire bonding. The out-of-plane component of the magnetization (M_z) of the nanostrips was measured by polar Kerr microscopy. An in-plane field of 200 mT along the current direction, combined with a 3 TA m⁻² current pulse was used to nucleate domains. Both MOKE and Kerr Microscopy characterization were performed using a 700 nm continuous wave laser in the polar configuration. Here, we chose the wavelength of the laser light ($\approx 700 \text{ nm}$) such that the detected signal is only sensitive to the magneto-optical response from the Co layer and Kerr rotation is maximized.

Supporting Information

Supporting Information is available from the Wiley Online Library or from the author.

Acknowledgements

This project has received funding from the European Union's Horizon 2020 research and innovation programme under the Marie Skłodowska-Curie grant agreement No.860060. This work is also part of the Gravitation programme "Research Centre for Integrated Nanophotonics", which is financed by the Netherlands Organisation for Scientific Research (NWO).

Conflict of Interest

The authors declare no conflict of interest.

Author Contributions

P.L. and T.J.K. contributed equally to this work in terms of design and conduct of the project. B.K. and R.L. supervised the project. All authors contributed to the writing of the manuscript.

Data Availability Statement

The data that support the findings of this study are available from the corresponding author upon reasonable request.

Keywords

all-optical switching, angular momentum compensation, current-induced domain wall motion, synthetic ferrimagnets

Received: June 27, 2022
Revised: September 25, 2022
Published online:

- [1] S. K. Kim, G. S. D. Beach, K.-J. Lee, T. Ono, T. Rasing, H. Yang, *Nat. Mater.* **2022**, 21, 24.
- [2] B. Dieny, I. L. Prejbeanu, K. Garello, P. Gambardella, P. Freitas, R. Lehndorff, W. Raberg, U. Ebels, S. O. Demokritov, J. Akerman, A. Deac, P. Pirro, C. Adelmann, A. Anane, A. V. Chumak, A. Hirohata, S. Mangin, S. O. Valenzuela, M. C. Onbasli, M. d'Aquino, G. Prenat, G. Finocchio, L. Lopez-Diaz, R. Chantrell, O. Chubykalo-Fesenko, P. Bortolotti, *Nat. Electron.* **2020**, 3, 446.
- [3] S. S. P. Parkin, M. Hayashi, L. Thomas, *Science* **2008**, 320, 190.
- [4] D. Kumar, T. Jin, R. Sbiaa, M. Kläui, S. Bedanta, S. Fukami, D. Ravelosona, S.-H. Yang, X. Liu, S. Piramanayagam, *Phys. Rep.* **2022**, 958, 1.
- [5] R. Blaesing, A. A. Khan, P. C. Filippou, C. Garg, F. Hameed, J. Castrillon, S. S. P. Parkin, *Proc. IEEE* **2020**, 1.
- [6] I. M. Miron, T. Moore, H. Szabolcs, L. D. Buda-Prejbeanu, S. Auffret, B. Rodmacq, S. Pizzini, J. Vogel, M. Bonfim, A. Schuhl, G. Gaudin, *Nat. Mater.* **2011**, 10, 419.
- [7] K.-S. Ryu, L. Thomas, S.-H. Yang, S. Parkin, *Nat. Nanotechnol.* **2013**, 8, 527.
- [8] P. P. J. Haazen, E. Muré, J. H. Franken, R. Lavrijsen, H. J. M. Swagten, B. Koopmans, *Nat. Mater.* **2013**, 12, 299.
- [9] S.-H. Yang, K.-S. Ryu, S. Parkin, *Nat. Nanotechnol.* **2015**, 10, 221.
- [10] S. S. P. Parkin, *Phys. Rev. Lett.* **1991**, 67, 3598.
- [11] J. Yu, D. Bang, R. Mishra, R. Ramaswamy, J. H. Oh, H.-J. Park, Y. Jeong, P. Van Thach, D.-K. Lee, G. Go, S.-W. Lee, Y. Wang, S. Shi, X. Qiu, H. Awano, K.-J. Lee, H. Yang, *Nat. Mater.* **2019**, 18, 29.
- [12] L. Caretta, M. Mann, F. Buttner, K. Ueda, B. Pfau, C. M. Gunther, P. Helsing, A. Churikova, C. Klose, M. Schneider, D. Engel, C. Marcus, D. Bono, K. Bagschik, S. Eisebitt, G. S. D. Beach, *Nat. Nanotechnol.* **2018**, 13, 1154.
- [13] T. Okuno, D.-H. Kim, S.-H. Oh, S. K. Kim, Y. Hirata, T. Nishimura, W. S. Ham, Y. Futakawa, H. Yoshikawa, A. Tsukamoto, Y. Tserkovnyak, Y. Shiota, T. Moriyama, K.-J. Kim, K.-J. Lee, T. Ono, *Nat. Electron.* **2019**, 2, 389.
- [14] M. L. Alexey, V. Kimel, *Nat. Rev. Mater.* **2019**, 4, 189.
- [15] T. A. Ostler, J. Barker, R. F. L. Evans, R. W. Chantrell, U. Atxitia, O. Chubykalo-Fesenko, S. El Moussaoui, L. Le Guyader, E. Mengotti, L. J. Heyderman, F. Nolting, A. Tsukamoto, A. Itoh, D. Afanasiev, B. A. Ivanov, A. M. Kalashnikova, K. Vahaplar, J. Mentink, A. Kirilyuk, T. Rasing, A. V. Kimel, *Nat. Commun.* **2012**, 3, 666.
- [16] I. Radu, K. Vahaplar, C. Stamm, T. Kachel, N. Pontius, H. A. Durr, T. A. Ostler, J. Barker, R. F. L. Evans, R. W. Chantrell, A. Tsukamoto, A. Itoh, A. Kirilyuk, T. Rasing, A. V. Kimel, *Nature* **2011**, 472, 205.
- [17] A. R. Khorsand, M. Savoini, A. Kirilyuk, A. V. Kimel, A. Tsukamoto, A. Itoh, T. Rasing, *Phys. Rev. Lett.* **2012**, 108, 127205.
- [18] P. Li, M. J. G. Peeters, Y. L. W. van Hees, R. Lavrijsen, B. Koopmans, *Appl. Phys. Lett.* **2021**, 119, 252402.
- [19] J. H. Mentink, J. Hellsvik, D. V. Afanasiev, B. A. Ivanov, A. Kirilyuk, A. V. Kimel, O. Eriksson, M. I. Katsnelson, T. Rasing, *Phys. Rev. Lett.* **2012**, 108, 057202.
- [20] H. Becker, C. J. Kruckel, D. V. Thourhout, M. J. R. Heck, *IEEE J. Sel. Top. Quantum Electron.* **2020**, 26, 1.
- [21] E. K. Sobolewska, J. Pelloux-Prayer, H. Becker, G. Li, C. S. Davies, C. J. Kruckel, L. A. Felix, A. Olivier, R. C. Sousa, I. L. Prejbeanu, A. I. Kiriliouk, D. V. Thourhout, T. Rasing, F. Moradi, M. J. R. Heck, *Proc. SPIE* **2020**, 11461, 8.
- [22] M. L. M. Laliou, M. J. G. Peeters, S. R. R. Haenen, R. Lavrijsen, B. Koopmans, *Phys. Rev. B* **2017**, 96, 220411.
- [23] L. Wang, H. Cheng, P. Li, Y. Liu, Y. L. W. V. Hees, R. Lavrijsen, X. Lin, K. Cao, B. Koopmans, W. Zhao, *Proc. Natl. Acad. Sci.* **2022**, 119, e2204732119.
- [24] M. Beens, M. L. M. Laliou, R. A. Duine, B. Koopmans, *AIP Adv.* **2019**, 9, 125133.
- [25] L. Wang, Y. L. W. van Hees, R. Lavrijsen, W. Zhao, B. Koopmans, *Appl. Phys. Lett.* **2020**, 117, 022408.
- [26] M. L. M. Laliou, R. Lavrijsen, B. Koopmans, *Nat. Commun.* **2019**, 10, 110.
- [27] R. Blaesing, T. Ma, S.-H. Yang, C. Garg, F. K. Dejene, A. T. N'Diaye, G. Chen, K. Liu, S. S. P. Parkin, *Nat. Commun.* **2018**, 9, 4984.
- [28] K. Cai, Z. Zhu, J. M. Lee, R. Mishra, L. Ren, S. D. Pollard, P. He, G. Liang, K. L. Teo, H. Yang, *Nat. Electron.* **2020**, 3, 37.
- [29] E. A. Nesbitt, H. J. Williams, J. H. Wernick, R. C. Sherwood, *J. Appl. Phys.* **1962**, 33, 1674.
- [30] K.-J. Kim, S. K. Kim, Y. Hirata, S.-H. Oh, T. Tono, D.-H. Kim, T. Okuno, W. S. Ham, S. Kim, G. Go, Y. Tserkovnyak, A. Tsukamoto, T. Moriyama, K.-J. Lee, T. Ono, *Nat. Mater.* **2017**, 16, 1187.
- [31] L. Aviles-Felix, L. Alvaro-Gomez, G. Li, C. S. Davies, A. Olivier, M. Rubio-Roy, S. Auffret, A. Kirilyuk, A. V. Kimel, T. Rasing, L. D. Buda-Prejbeanu, R. C. Sousa, B. Dieny, I. L. Prejbeanu, *AIP Adv.* **2019**, 9, 125328.
- [32] Y. Yang, R. B. Wilson, J. Gorchon, C.-H. Lambert, S. Salahuddin, J. Bokor, *Sci. Adv.* **2017**, 3, e1603117.
- [33] M. Beens, M. L. M. Laliou, A. J. M. Deenen, R. A. Duine, B. Koopmans, *Phys. Rev. B* **2019**, 100, 220409.
- [34] I. M. Miron, K. Garello, G. Gaudin, P.-J. Zermatten, M. V. Costache, S. Auffret, S. Bandiera, B. Rodmacq, A. Schuhl, P. Gambardella, *Nature* **2011**, 476, 189.
- [35] A. Thiaville, J. M. Garcia, J. Miltat, *J. Magn. Magn. Mater.* **2002**, 242-245, 1061.
- [36] A. V. Svalov, A. Fernandez, V. O. Vas'kovskiy, M. Tejedor, J. M. Barandiaran, I. Orue, G. V. Kuryandskaya, *J. Magn. Magn. Mater.* **2006**, 304, e703.
- [37] E. Martinez, S. Emori, N. Perez, L. Torres, G. S. D. Beach, *J. Appl. Phys.* **2014**, 115, 213909.
- [38] S. A. Siddiqui, J. Han, J. T. Finley, C. A. Ross, L. Liu, *Phys. Rev. Lett.* **2018**, 121, 057701.